



Utilizing Interferometric Synthetic Aperture Radar and Ground-Based Radar Data to Predict Time to Failure and to Calibrate Numerical Models on an Opencast Coal Mine

Jacques Strydom¹(✉) and Ohveshlan Pillay²

¹ New Vaal Colliery, Vereeniging, South Africa
Jacques.strydom@seritiza.com

² University of the Witwatersrand, Johannesburg, South Africa

Abstract. Accurate time failure predictions and improved geotechnical certainty in an opencast mine will lead to tremendous safety and economic benefits. This study utilizes interferometric synthetic aperture radar and ground-based radar data to conduct a back analysis on slope failures that have occurred in an opencast coal mine in South Africa. Time to failure predictions was done utilizing the inverse velocity technique, while the effect of different data smoothing techniques on the accuracy of the failure predictions was evaluated. Additionally, ground-based radar data was used to calibrate a finite element numerical model to improve geotechnical certainty. Time to failure predictions based on satellite monitoring data was less accurate than predicted in the literature. This study confirms that displacement measurement from ground-based radars may be used to optimize the strength parameters of finite element numerical models. To improve the accuracy of time to failure predictions from satellite monitoring data, it was proposed that a satellite constellation with a shorter data acquisition time must be utilized. By having access to more frequent data acquisitions and by identifying the most active points within the failure zone of a slope, it is expected that the accuracy of the time to failure predictions can be improved.

Keywords: InSAR · Inverse Velocity · Finite Element Numerical Modelling

1 Introduction

The devastating consequences of slope failures necessitate the proactive management of slope stability. Slope stability management involves the design, construction, and monitoring of excavated slopes. To eliminate the potential loss of life and minimize the damage to equipment and production time losses in opencast mines, accurate time to failure predictions is required [1, 9]. To accurately predict the time to failure, a method is required to measure the location and rate of displacement on slopes. The combination of ground-based radar and InSAR monitoring proved to be highly effective in monitoring displacement on slopes to predict their expected time to failure [2, 10].

© The Author(s) 2023

R. E. Hammah et al. (Eds.): RIC 2023, AHE 19, pp. 191–198, 2023.

https://doi.org/10.2991/978-94-6463-258-3_20

During the design phase of rock slopes, a stability analysis is required to obtain a safety factor (SF) and probability of failure (POF) of the slope. This can be done by conducting stability analysis with numerical modelling software [7]. The material properties used in the numerical modelling software are usually obtained from laboratory tests and can be refined by conducting a probabilistic back analysis when a failure occurs [6]. Alternatively, ground-based radar data and InSAR data can be utilized to calibrate and refine sophisticated three-dimensional (3D) and two-dimensional (2D) numerical models [5, 8, 12].

This paper will discuss the utilization of satellite InSAR monitoring data to evaluate its ability to predict the time to failure of slopes on an opencast coal mine. Additionally, the potential of using ground-based radar data to calibrate a finite element numerical model to improve geotechnical certainty will be covered.

2 Methodology

Five historic slope failures were identified on an operational open-cast strip mine. A back analysis of the failures was conducted to evaluate the effectiveness of InSAR to predict the time to failure of slopes, utilizing the inverse velocity technique. Additionally, the displacement measured by a real aperture ground-based radar was compared to the displacement predicted by finite element models to calibrate the material properties used.

2.1 Data Acquisition and Numerical Modeling

SkyGeo assisted with the back analysis of five historic slope failures at Seriti's New Vaal Colliery, using InSAR to measure millimeter scale displacements. The data acquired originated from Sentinel-1 ascending orbital track T116 and descending orbital track T50. The satellite acquires new data over the same area, once every 12 days during each orbital repeat. The line of sight displacement data was made available on an online viewer, displayed on either low-resolution satellite images or high-resolution digital elevation models supplied by the mine.

Ground-based radar data was obtained from Reutech's MSR300 trailer-mounted real aperture radar and numerical modelling was done with Rocscience's RS2.

2.2 Inverse Velocity Plots and Data Smoothing

Two time to failure predictions were done for every failure. The first prediction was based on the average movement detected on all the radar points included within the failure boundary. For the second time to failure prediction, a cluster of highly active points within the failure boundary was manually identified to improve the failure prediction accuracy as proposed in the literature [4].

Data smoothing was done in Microsoft Excel using Eqs. 1 and 2. The moving average and exponential smoothing algorithms are commonly used for noise clean-up and data smoothing [1]. A short-term simple moving average (SMA), where the smoothed velocity, v_t , at a time, t , can be calculated with Eq. 1.

$$v_t = \frac{v_t + v_{t-1} + \dots + v_{t-(n-1)}}{n} \quad (1)$$

where $n = 3$.

An exponential smoothing function (ESF) can be calculated with Eq. 2.

$$v_t = \beta \cdot v_t + (1 - \beta) \cdot v_{t-1} \quad (2)$$

where the smoothing factor $\beta = 0.5$.

Inverse velocity plots were not applied from the true onset of acceleration (OOA). As proposed in the literature, the prediction was applied from the point preceding the failure that gave the highest regression line (R^2) value. This was typically the last four to seven measurement points before the failure [3].

3 Results and Discussion

3.1 Time to Failure Prediction Accuracy and Data Smoothing Techniques

The accuracy of inverse velocity time to failure predictions is extremely variable and relies significantly on both measurement noise and the data smoothing technique that has been applied. As predicted by the literature, the inverse velocity plots were especially sensitive to the influence of noise when working with low velocities [1].

When evaluating the time to failure prediction accuracy, based on InSAR data with a 12-day data acquisition time, it is important to keep in mind that a significant percentage of the overall slope displacement occurs in the final hours before the failure. A clear correlation was observed between the accuracy of the failure prediction and the closer the last measurement was taken before the failure.

The size of the failure also has a significant influence on the length of the pre-failure deformation phase. Larger failures tend to show longer phases of precursor deformation [1]. In general, slope failures in coal mines are significantly smaller in size compared to landslides and slope failures in massive opencast mines.

The linear fit of the regression line is an indication of the quality of the data, and a regression line value of between 0.7 to 0.9 is considered to be of sufficient quality for the predictions [9]. Due to the excessive noise in the data, numerous failure predictions could not satisfy this requirement and were, therefore, excluded when the averages of the failure accuracies and regression line values were calculated.

The predicted failure times and regression line values are summarized in Table 1 and Table 2. By excluding the failures that had been affected by external influences such as excessive rain or mechanical unconfinement and the regression line values that were below 0.7, an average failure accuracy was calculated for the different smoothing techniques.

The ESF resulted in more accurate time to failure predictions than the SMA (refer to Table 2). The poor regression line values were due to the high degree of noise included in the satellite data. Contrary to what had been found in the literature, the ESF resulted in a better fit to the regression line than the SMA [1]. This might be because the datasets that were analyzed for this project, in general, included an excessive amount of noise. Positive values indicate a predicted failure date after the actual failure and negative values indicate a predicted failure date before the actual failure date in Table 1.

Table 1. Difference between actual and predicted failure dates. Positive values indicate a predicted failure date after the actual failure and negative values indicate a predicted failure date before the actual failure date

Failure Date	SMA	ESF	Radar Points	Comments	Acquisition*
21-Jun-21	+163.25	+130.35	Whole Area	External influence	7 days
21-Jun-21	+19.99 [†]	+4.26	Active Points	External influence	7 days
30-Apr-21	-8.73	-3.48	Whole Area	Usable data	0 days
30-Apr-21	-4.82	+0.92	Active Points	Usable data	0 days
01-Jan-21	+13.57 [†]	+141.1 [†]	Whole Area	External influence	3 days
01-Jan-21	+5.77	+60.91 [†]	Active Points	External influence	3 days
22-Oct-20	-38.41	-40.71 [†]	Whole Area	Usable data	9 days
22-Oct-20	-5.37	-13.86	Active Points	Usable data	9 days
30-Mar-19	-14.94 [†]	-33.71 [†]	Whole Area	Noise	5 days
30-Mar-19	-15.36 [†]	-17.90	Active Points	Usable data	5 days

[†]Regression line value below 0.7. Data is not valid

*Time difference between the last acquisition date and actual failure date

Table 2. Summary of regression line values

	30-Mar-19	22-Oct-20	01-Jan-21	30-Apr-21	21-Jun-21	Average	Poor Fit	Accuracy (days)
SMA (WA)*	0.23	0.79	0.68	0.80	0.80	0.66	2	23.57
SMA (AP)**	0.52	0.94	0.73	0.75	0.21	0.63	2	5.10
ESF (WA)*	0.54	0.53	0.53	0.95	0.94	0.70	3	3.48
ESF (AP)**	0.74	0.99	0.64	0.92	0.92	0.84	1	10.76

*WA – All radar points included in the failure zone

** AP – Only the most active radar points within the failure zone

The inaccurate failure dates might be explained by the fact the failure predictions were not applied from a true OOA point as proposed in the literature [11]. Furthermore, the low deformation values recorded result in the predictions being severely affected by noise that cannot necessarily be filtered out. Except for the time to failure prediction for the highwall failure that occurred on 30 April 2021, based on the most active radar points, and smoothed with the ESF, all the valid inverse plots indicated a predicted failure date before the actual failure date.

Based on the literature, it was expected that the accuracy of the failure prediction should improve the closer the last measurement was taken before the actual failure date [3]. This was observed from the time to failure predictions that had no external influences. The most accurate prediction had a measurement hours before the actual failure. By utilizing satellites with shorter revisit times, the accuracy of time to failure predictions should be improved.

3.2 Numerical Modelling Results

By utilizing the displacement monitoring data from the ground-based radar the accuracy of the predicted displacement and failure location of the model was improved. By reducing the strength parameters used in the model by 6%, the displacement predicted by the finite element model in Fig. 1 correlates well with the displacement measured by the ground-based radar at the time of failure Fig. 2. The model predicted a displacement of 16 mm at the time of failure, while the actual displacement measured at the time of failure was 15.6 mm. Take note that the assumption is made that the spoil creep that preceded the failure can be ignored. The measured displacement was focused on the actual material that failed.

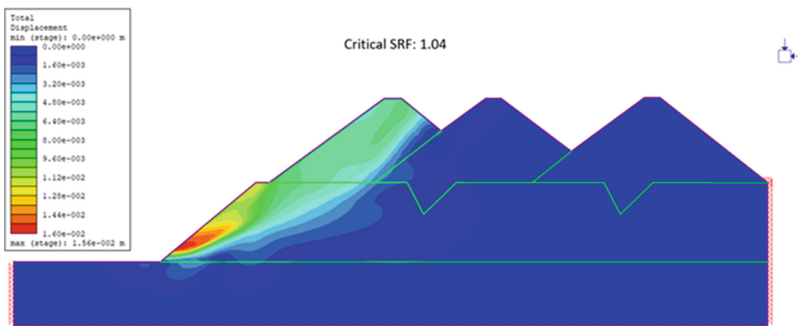


Fig. 1. RS2 finite element model predicting 16 mm displacement at a safety factor of 1.04

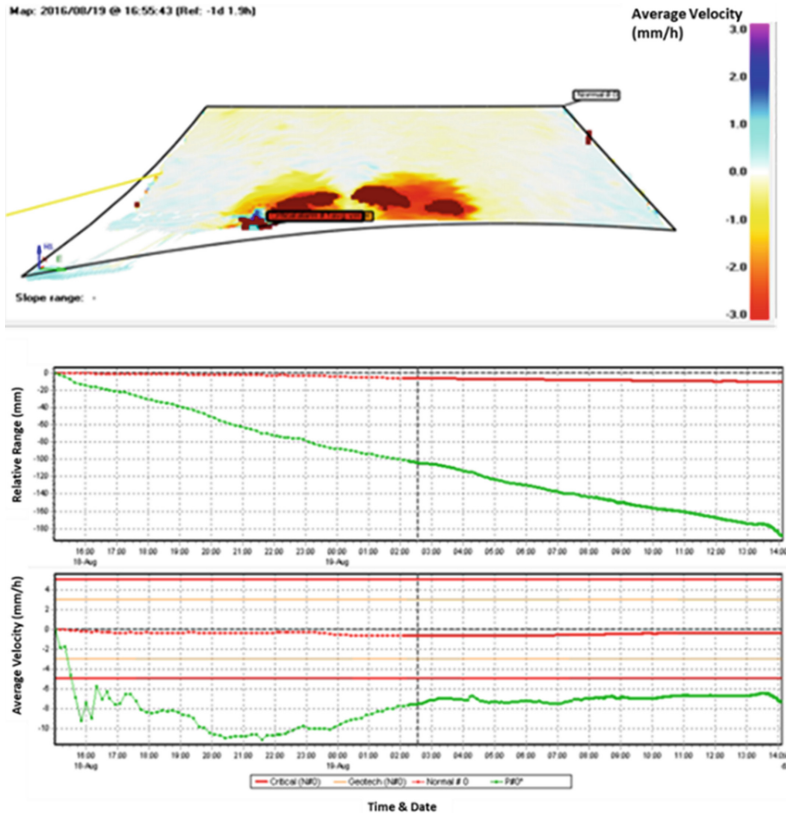


Fig. 2. Displacement of 15.6 mm measured by the ground-based radar at the time of failure

4 Conclusion

4.1 Time to Failure Predictions

The average error of the time to failure predictions ranged from 3.48 to 23.57 days, a significantly larger margin of error than a couple of hours reported in the literature. The accuracy of time to failure predictions based on InSAR data must improve to add real value to mining operations. This may be achieved by improving data processing to remove the noise and by utilizing satellites with shorter revisit times. Time to failure predictions that are several days out will negatively impact production and safety in the mine. It was observed that the accuracy of the failure predictions did improve the closer the last measurement was taken to the actual failure date. External influences such as mechanical unconfinement, excessive rain and pre-existing planes of weaknesses must all be considered when attempting to predict the time to failure. The most accurate time to failure prediction was for a circular failure that occurred in sand material which had no external influences and limited measurement noise. Time to failure predictions should still only be used as a guideline and a reasonable factor of safety should be used when

utilizing the inverse velocity technique to prolong production underneath a potentially unstable slope.

4.2 Numerical Model Calibration

Strength parameters from laboratory data will remain a logical starting point for numerical models, but the utilization of radar data does have the ability to improve the accuracy of the numerical models and reduce geotechnical uncertainty. The displacement measured directly before the failure by the ground-based radar correlated well with the magnitude and position of the displacement predicted by the finite element model. The original strength parameters of the site had to be decreased by 6% to achieve this. It increased the confidence in the numerical model, as it was a close representation of what was observed in the pit.

4.3 Recommendations

It is recommended that the utilization of InSAR data to predict time to failure on strip mines needs to be investigated further. A target site must be identified and actively monitored with a combination of satellites such as TerraSAR-x and PAZ to improve data acquisition times. The use of an automatic slope failure prediction model, which automatically identifies the most active points on a slope and does automatic time to failure predictions as new data is acquired, is also recommended.

References

1. Carlà, T., Intrieri, E., Di Traglia, F., Nolesini, T., Gigli, G. & Casagli, N. 2017. Guidelines on the use of inverse velocity method as a tool for setting alarm thresholds and forecasting landslides and structure collapses. *Landslides*. 14(2):517–534. DOI: <https://doi.org/10.1007/s10346-016-0731-5>.
2. Carlà, T., Farina, P., Intrieri, E., Ketizmen, H. & Casagli, N. 2018. Integration of ground-based radar and satellite InSAR data for the analysis of an unexpected slope failure in an open-pit mine. *Engineering Geology*. 235(September 2017):39–52. DOI: <https://doi.org/10.1016/j.enggeo.2018.01.021>.
3. Carlà, T., Intrieri, E., Raspini, F., Bardi, F., Farina, P., Ferretti, A., Colombo, D., Novali, F., et al. 2019. Perspectives on the prediction of catastrophic slope failures from satellite InSAR. *Scientific Reports*. 9(1):1–9. DOI: <https://doi.org/10.1038/s41598-019-50792-y>.
4. Dick, G.J., Eberhardt, E., Cabrejo-Liévano, A.G., Stead, D. & Rose, N.D. 2015. Development of an early-warning time-of-failure analysis methodology for open-pit mine slopes utilizing ground-based slope stability radar monitoring data. *Canadian Geotechnical Journal*. 52(4):515–529. DOI: <https://doi.org/10.1139/cgj-2014-0028>.
5. Escobar, A., Farina, P., Leoni, L., Iasio, C. & Coli, N. 2013. Innovative use of slope monitoring radar as a support to geotechnical modelling of slopes in open pit mines. 793–801. DOI: https://doi.org/10.36487/acg_rep/1308_54_farina.
6. Jagriti Mandal, Sruti Narwal & Dr. S. S. Gupte. 2017. Back Analysis of Failed Slopes - A Case Study. *International Journal of Engineering Research and*. V6(05). DOI: <https://doi.org/10.17577/ijertv6is050366>.

7. Kanda, M.J. & Stacey, T.R. 2016. The influence of various factors on the results of stability analysis of rock slopes and on the evaluation of risk. *Journal of the Southern African Institute of Mining and Metallurgy*. 116(11):1075–1081. DOI: <https://doi.org/10.17159/2411-9717/2016/v116n11a10>.
8. McQuillan, A., Yacoub, T., Bar, N., Coli, N., Leoni, L., Rea, S. & Bu, J. 2020. Three-dimensional slope stability modelling and its interoperability with interferometric radar data to improve geotechnical design. In *Proceedings of the 2020 International Symposium on Slope Stability in Open Pit Mining and Civil Engineering*. Australian Centre for Geomechanics, Perth. 1349–1358. DOI: https://doi.org/10.36487/ACG_repo/2025_92.
9. Osasan, K.S. & Stacey, T.R. 2014. Automatic prediction of time to failure of open pit mine slopes based on radar monitoring and inverse velocity method. *International Journal of Mining Science and Technology*. 24(2):275–280. DOI: <https://doi.org/10.1016/j.ijmst.2014.01.021>.
10. Paradella, W.R., Ferretti, A., Mura, J.C., Colombo, D., Gama, F.F., Tamburini, A., Santos, A.R., Novali, F., et al. 2015. Mapping surface deformation in open pit iron mines of Carajás Province (Amazon Region) using an integrated SAR analysis. *Engineering Geology*. 193:61–78. DOI: <https://doi.org/10.1016/j.enggeo.2015.04.015>
11. Rose, N.D. & Hungr, O. 2007. Forecasting potential rock slope failure in open pit mines using the inverse-velocity method. *International Journal of Rock Mechanics and Mining Sciences*. 44(2):308–320. DOI: <https://doi.org/10.1016/j.ijrmms.2006.07.014>.
12. Woo, K.S., Eberhardt, E., Rabus, B., Stead, D. & Vyazmensky, A. 2012. Integration of field characterisation, mine production and InSAR monitoring data to constrain and calibrate 3-D numerical modelling of block caving-induced subsidence. *International Journal of Rock Mechanics and Mining Sciences*. 53:166–178. DOI: <https://doi.org/10.1016/j.ijrmms.2012.05.008>.

Open Access This chapter is licensed under the terms of the Creative Commons Attribution-NonCommercial 4.0 International License (<http://creativecommons.org/licenses/by-nc/4.0/>), which permits any noncommercial use, sharing, adaptation, distribution and reproduction in any medium or format, as long as you give appropriate credit to the original author(s) and the source, provide a link to the Creative Commons license and indicate if changes were made.

The images or other third party material in this chapter are included in the chapter's Creative Commons license, unless indicated otherwise in a credit line to the material. If material is not included in the chapter's Creative Commons license and your intended use is not permitted by statutory regulation or exceeds the permitted use, you will need to obtain permission directly from the copyright holder.

